Fluctuation Conductivity of $RE_{1-2x}Ca_xM_xBa_2Cu_3O_{7-\delta}$ (RE=Nd, Y and M=Pr, Th) Superconductors

S. R. Ghorbani & M. Rahmati Tarki

Journal of Superconductivity and Novel Magnetism
Incorporating Novel Magnetism

ISSN 1557-1939
Volume 27
Number 3

J Supercond Nov Magn (2014)
27:749-754
DOI 10.1007/s10948-013-2381-3

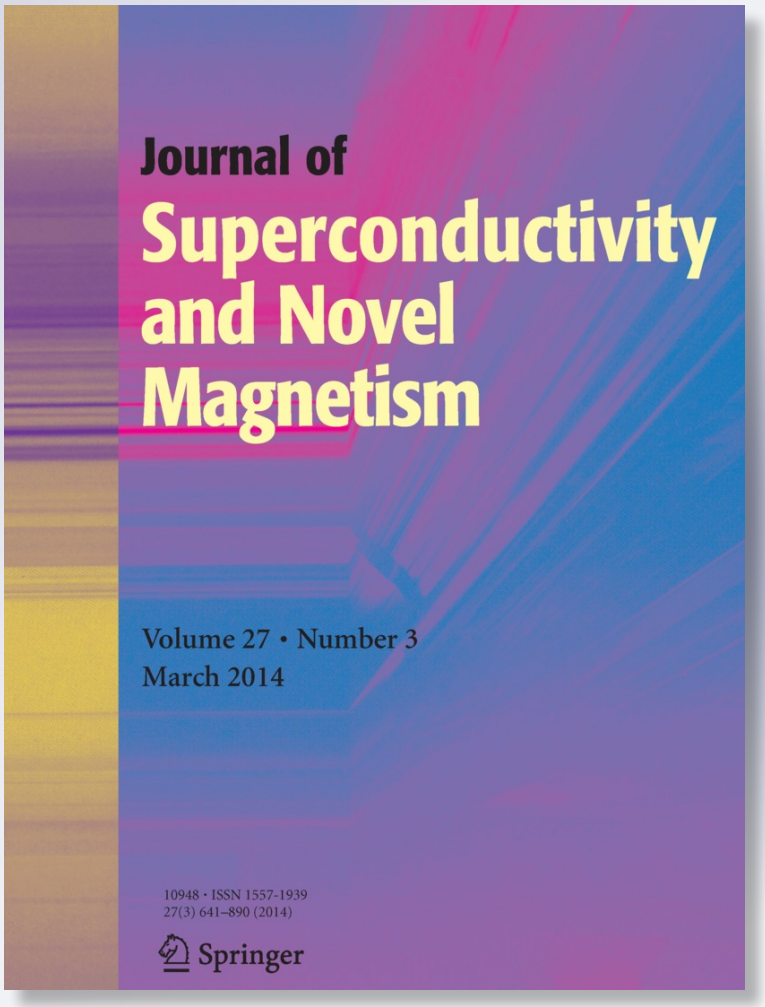

Springer

J Supercond Nov Magn (2014) 27:749–754
DOI 10.1007/s10948-013-2381-3

ORIGINAL PAPER

Fluctuation Conductivity of $RE_{1-2x}Ca_xM_xBa_2Cu_3O_{7-\delta}$ (RE = Nd, Y and M = Pr, Th) Superconductors

S.R. Ghorbani · M. Rahmati Tarki

Received: 17 May 2013 / Accepted: 7 August 2013 / Published online: 4 October 2013

Abstract Polycrystalline samples of $RE_{1-2x}Ca_xM_xBa_2Cu_3O_{7-\delta}$ with RE = Nd, Y and M = Pr, Th (with $0.0 \leq x \leq 0.10$), superconductors were prepared by the standard solid-state method. Resistivity was measured as a function of temperature and doping concentration x. Excess conductivity was analyzed using the modified Lawrence-Doniach (LD) expressions. The fluctuation regions, crossover temperatures, coherence lengths, and effective layer thickness were obtained and the values were compared for both samples. For both samples, it was found that with increasing doping, the crossover temperatures were reduced, while the coherence length decreased. The upper critical field and critical current density were increased with increasing doping concentration due to the introduction of disorder and the enhancement of flux pinning by charge neutral doping. Furthermore, the coherence lengths of the Nd-based samples are larger than that for the Y-based samples by a factor 2. It was found that the value of critical current density in Nd(CaPr)-123 is higher than Y(CaTh)-123, from which it is suggested that CaPr doping is more effective than CaTh doping.

Keywords Superconductivity · Fluctuation · Excess conductivity

S.R. Ghorbani (✉)
Department of Physics, Ferdowsi University of Mashhad, Mashhad, Iran
e-mail: sh.ghorbani@um.ac.ir

M. Rahmati Tarki
Department of Physics, Hakim Sabzevari University, Sabzevar, Iran

1 Introduction

Since the discovery of the high-critical-temperature (high T_c) cuprate superconductors [1], a large number of studies have been performed to understand the mechanism of high-T_c superconductivity. In spite of many efforts, however, the mechanism of high-T_c superconductivity still remains unclear. The observed deviation from the linear relation between resistivity and temperature above T_c in high-temperature superconductors, which is called excess conductivity, has been explained on the basis of fluctuations in the superconducting order parameter. The Cooper pairs are simultaneously formed and broken as the temperature approaches T_c. The formation of these Cooper pairs may give rise to excess conductivity of the carriers.

There are two main sources of excess conductivity. The first is the formation of Cooper pairs above the critical temperature, arising from the fluctuation-induced conductivity, as given by the Aslamasov-Larkin (AL) contribution [2], which is explained by the Lawrence-Doniach (LD) model [3]. It predicts a crossover from the three-dimensional (3D) electronic state of the system to the two-dimensional (2D) state with increasing temperature. In oxide superconductors, the AL term dominates close to T_c. The second source of excess conductivity relates to the effect of superconducting fluctuations on the conductivity of normal electrons, given by the Maki-Thompson (MT) contribution [4, 5]. The MT term depends largely on the phase-relaxation time, t_φ, and becomes important in the 2D fluctuation regime with moderate pair-breaking [6]. The study of excess conductivity due to thermodynamic fluctuation provides useful information on some of the fundamental aspects, such as understanding the intrinsic superconducting characteristics and the dimensionality of high-T_c systems. There have been several models of the excess conductivity,

such as the Aslamasov and Larkin (AL), Lawerence and Doniach (LD), and Varlamov and Livanov (VL) models [7–11].

It is well known that non-isovalent atomic substitution has two main effects on the solid structure. The first is the addition of carriers to the lattice, and the second is disorder introduced by doping. The way to study these effects separately is by using charge neutral doping. The neutral doping enables one to infer the main effects of disorder on various normal and superconducting state properties, since electrons (holes) added to the lattice are compensated by added holes (electrons).

In the present paper we have studied the excess conductivity in polycrystalline $Nd_{1-2x}Ca_xPr_xBa_2Cu_3O_{7-\delta}$ and $Y_{1-2x}Ca_xTh_xBa_2Cu_3O_{7-\delta}$ samples with $0.00 \leq x \leq 0.10$. The effects of the doping on superconductivity parameters such as the coherence length, the upper critical field, and the critical current density have been investigated by the modified Lawrence-Doniach model. Results show that the upper critical field and critical current density were increased with increasing dopant concentration, due to the introduction of disorder by increasing charge neutral doping.

2 Experimental

Samples of $Nd_{1-2x}Ca_xPr_xBa_2Cu_3O_{7-\delta}$ and $Y_{1-2x}Ca_xTh_xBa_2Cu_3O_{7-\delta}$ with $0.00 \leq x \leq 0.10$ were prepared by standard solid-state methods. Starting materials were high-purity RE_2O_3 (RE = Y, Nd), $BaCO_3$, CuO, $CaCO_3$ and Th_2O_3, and Pr_6O_{11}. The samples were pressed into pellets and calcined in air at 900, 920, and 920 °C, respectively, with intermediate grindings. Annealing was then performed in flowing oxygen at 460 °C for 3 days, and the temperature was finally decreased to room temperature at a slow rate of 12 °C/h. X-ray diffraction (XRD) patterns were recorded by a Guinier-Hagg focusing camera using CuK_α radiation with Si as an internal standard. The electrical resistivity was measured with a standard dc four-probe method. Electrical leads were attached to the sample by silver paint and heat treated at 300 °C in flowing oxygen for half an hour, which gave contact resistance of the order of 1–2 Ω [12].

3 Theoretical Considerations

The excess conductivity due to superconductivity fluctuation behavior was obtained from [13]:

$$\Delta\sigma = \sigma(T) - \sigma_n(T) \tag{1}$$

where $\sigma(T) = 1/\rho(T)$ is the measured conductivity and $\sigma_n(T) = 1/\rho_n(T)$ is the extrapolated conductivity fitted with $\rho_n = \rho(0) + aT$, where $\rho(0)$ is the residual resistivity at $T = 0$ (intercept) and a is the slope of the resistivity *vs*. temperature relation.

Aslamasov-Larkin [14] obtained the following expression for describing the excess conductivity using a microscopic approach in the mean field region (MFR), where the fluctuations are small:

$$\frac{\Delta\sigma}{\sigma_{300}} = A\varepsilon^{-\lambda} \tag{2}$$

where the reduced temperature $\varepsilon = (T - T_{mf})/T_{mf}$. T_{mf} is the mean field temperature given by the peak in the $d\rho/dT$ versus T plot. λ is the conductivity exponent, which equals -0.5 for the 3D region, -1 for the 2D region, and -1.5 for the 1D region fluctuations. σ_{300} is the room-temperature conductivity. A is an independent constant, which is given by [15, 16]

$$A = \begin{cases} \frac{e^2}{32\hbar\xi_c(0)\sigma_{300}} & \text{for 3D fluctuation} \\ \frac{e^2}{16\hbar d\sigma_{300}} & \text{for 2D fluctuation} \\ \frac{e^2\xi_c(0)}{32\hbar s\sigma_{300}} & \text{for 1D fluctuation} \end{cases} \tag{3}$$

$\xi_c(0)$ is the zero-temperature coherence length along the c-axis, d is the effective layer thickness of the 2D system, and s is the cross-sectional area of the 1D system.

The dimensionality of the critical fluctuation (D) is $D = 2(2 + \lambda)$. The physical parameters calculated from fluctuation-induced conductivity (FIC) analysis depend strongly on the dimensionality of the fluctuations. The crossover from 2D to 3D is mainly found above the critical temperature. A characteristic temperature, T_0, is obtained, which is called the crossover temperature. The system has 3D fluctuations below this temperature and 2D fluctuations above this temperature, which can be explained by the AL equations. The expression for the crossover temperature according to the LD model [3, 17] is

$$T_0 = T_c\left\{1 + \left[\frac{2\xi_c(0)}{d}\right]^2\right\} \tag{4}$$

T_c is the critical temperature. The FIC analysis carried out by using the AL equations [2] is valid for single crystals, but its validity for the polycrystalline samples is limited. However, for the case of polycrystalline samples, Lawrence and Doniach [3, 18] proposed a modified expression for the AL equation, and their equations for 2D and 3D fluctuations are

$$\Delta\sigma_{2D} = \frac{1}{4}\left\{\frac{e^2}{16\hbar d}\varepsilon^{-1}\left[1 + \left(1 + \frac{8\xi_c^4(0)}{d^2\xi_{ab}^2(0)}\varepsilon^{-1}\right)^{\frac{1}{2}}\right]\right\} \tag{5}$$

$$\Delta\sigma_{3D} = \frac{e^2}{32\hbar\xi_p(0)}\varepsilon^{-\frac{1}{2}} \tag{6}$$

where ξ_{ab} is the coherence length in the ab plane and $\xi_p(0)$ is the effective characteristic coherence length given by

$$\frac{1}{\xi_p(0)} = \frac{1}{4}\left[\frac{1}{\xi_c(0)} + \left(\frac{1}{\xi_c^2(0)} + \frac{8}{\xi_{ab}^2(0)}\right)^{\frac{1}{2}}\right] \tag{7}$$

Table 1 The λ(3D), λ(2D), λ(1D), T^{cr-3D}, T^{3D-2D}, T^{2D-1D} and T_{mf} for $Nd_{1-2x}Ca_xPr_xBa_2Cu_3O_{7-\delta}$ and $Y_{1-2x}Ca_xTh_xBa_2Cu_3O_{7-\delta}$

	x	λ(3D)	λ(2D)	λ(1D)	T^{cr-3D} (K)	T^{3D-2D} (K)	T^{2D-1D} (K)	T_{mf} (K)	T_c (K)	ρ_0 (mΩ.cm)	d (nm)	J
Nd(CaPr)	0.00	−0.48	−1.04	−1.44	92.8	106.5	108.7	91.3	92.1	0.31	4.36	0.473
	0.050	−0.51	−1.02	−1.52	86.3	102.4	106.2	84	85.4	0.47	3.27	0.594
	0.10	−0.53	−0.98	−1.51	79.2	94.5	104.4	72.5	74.1	0.65	2.50	0.772
Y(CaTh)	0.00	−0.67	−0.01	−1.58	92.4	97.6	99.8	92.2	91.2	0.20	11.37	0.158
	0.025	−0.59	−1.12	−1.59	89.8	93.7	97.9	87.8	87.7	0.41	9.63	0.178
	0.050	−0.63	−1.08	−1.61	88.7	92.2	96.2	83.5	85.2	0.67	8.17	0.223
	0.075	−0.61	−1.05	−1.65	85.8	89.1	93.7	79.2	82.4	0.74	8.96	0.171

By assuming the highly anisotropic nature of the sample and using Eqs. (6) and (7), the crossover temperature is given by

$$T_0 = T_c\left[1 + \frac{\xi_p^2(0)}{d^2}\left(1 + \frac{\xi_p^2(0)}{16\xi_{ab}^2(0)}\right)\right] \tag{8}$$

Because the samples are polycrystalline, we have employed the above formulation to analyze the excess conductivity data, which is induced by fluctuation.

4 Results and Discussion

The temperature dependence of the electrical resistivity for $Nd_{1-2x}Ca_xPr_xBa_2Cu_3O_{7-\delta}$ ($x = 0.00, 0.050, 0.10$) and $Y_{1-2x}Ca_xTh_xBa_2Cu_3O_{7-\delta}$ ($x = 0.00, 0.025, 0.050, 0.075$) is shown in Fig. 1. Linear resistivity was observed in the normal state for all samples. On increasing the substitution content x, the resistivity curve is shifted upwards, indicating an increase of ρ_0 with x. This means that the primary scattering effect of the doping enhances the residual resistivity. The mean field temperature T_{mf} was obtained from the $d\rho/dT$ versus T plot (see inset Fig. 1). T_c is the critical temperature, which is defined from the midpoint of the resistive transition (50 % ρ_n) and the T_{mf} values are listed in Table 1.

Figure 2 shows the normalized excess conductivity $\Delta\sigma/\sigma_{room}$ versus the reduced temperature ε in a log-log plot. Four different fluctuation regions are clearly distinguishable, which can be identified as the critical, 3D, 2D, and 1D regions. Similar results were obtained by Abou-Aly et al. [13] in $Tl_{0.8}Hg_{0.2}Ba_2Cu_3O_{9-\delta}$ and Han et al. [21] in $Hg_{0.8}Tl_{0.2}Ba_2Cu_3O_{8+\delta}$. In order to compare the experimental data with theoretical predictions, the different regions are linearly fitted, and the conductivity exponent λ values are determined from the slopes. The obtained results for λ are listed in Table 1.

The 2D fluctuation conductivity is the contribution of the CuO_2 planes, which has been confirmed in RE-123 superconductors, where RE is a rare earth [19, 20]. The appearance of the 1D fluctuation conductivity suggests the existence of 1D conductivity channels, which may represent the

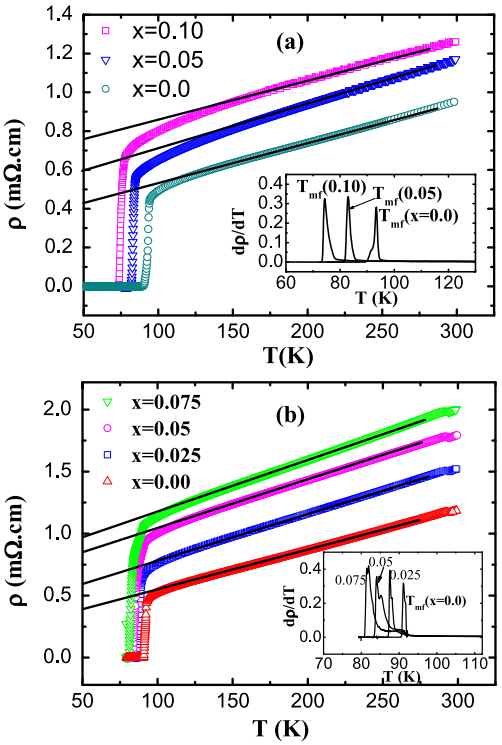

Fig. 1 The variation of electrical resistivity with T for (**a**) $Nd_{1-2x}Ca_xPr_xBa_2Cu_3O_{7-\delta}$ and (**b**) $Y_{1-2x}Ca_xTh_xBa_2Cu_3O_{7-\delta}$. *Inset*: $d\rho/dT$ versus T

CuO_x contribution to the conduction in the RE-123 superconductors. The 1D fluctuation conductivity in the cuprate superconductors would have a significant effect on our understanding of the superconducting process in these materials. The mean field region that is shown in the plots for each sample consists of two distinct linear parts, the 3D and the 2D regions.

It can be seen that the 3D region is shifted to lower temperature, and its width is decreased with the increasing doping. The crossover temperatures from the critical region to 3D, 3D to 2D, and 2D to the 1D region are decreased by increasing doping. The values determined for the crossover temperatures are listed in Table 1.

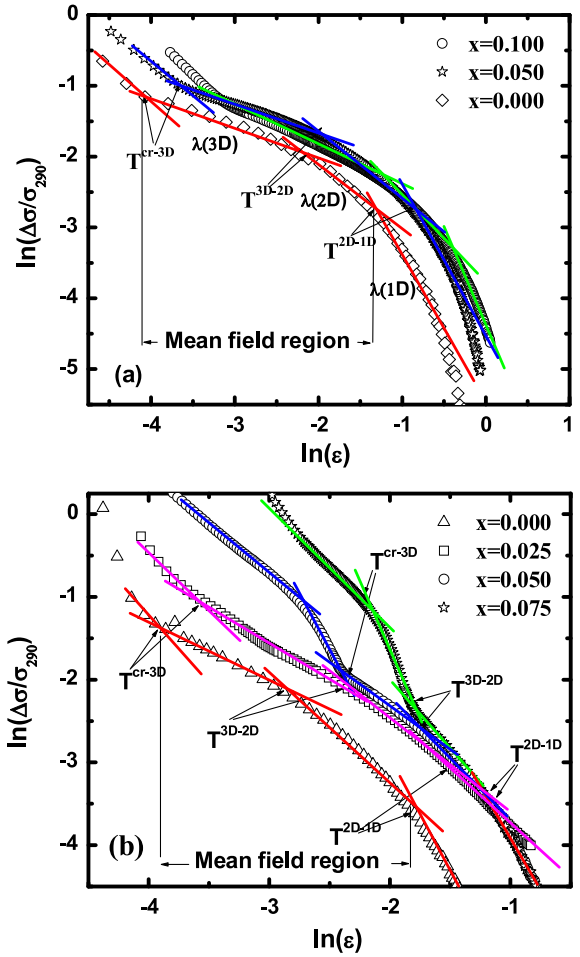

Fig. 2 $\ln(\Delta\sigma/\sigma_{\text{room}})$ versus $\ln(\varepsilon)$ plot for (**a**) $Nd_{1-2x}Ca_xPr_xBa_2Cu_3O_{7-\delta}$ and (**b**) $Y_{1-2x}Ca_xTh_xBa_2Cu_3O_{7-\delta}$

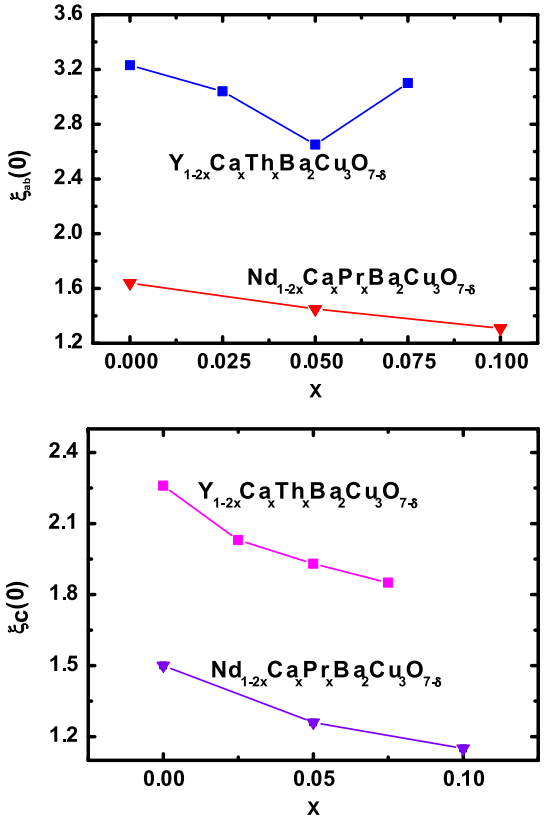

Fig. 3 The normalized coherence length versus x in the ab and c directions

The effective coherence length and the effective layer thickness were obtained by using Eqs. (5) and (6). The effective layer thickness results are given in Table 1. Then, the coherence lengths in the ab and c directions were calculated by using Eqs. (7) and (8). The results are shown in Fig. 3. By increasing the doping level, more disorder is introduced into the lattice, and the mean free path of electrons decreases, which results in a decreasing coherence length. The results for $x = 0.075$ in the $Y_{1-2x}Ca_xTh_xBa_2Cu_3O_{7-\delta}$ sample do not obey this increasing process and decrease, because the limit of solution in the solid state for CaTh is less than 0.075 [22]. As can be seen in Fig. 3, the coherence length in Nd(CaPr)-123 compound is smaller than that in Y(CaTh)-123. Therefore, the mean free path of electrons in the first compound is smaller than second one because it is proportional to the coherence length. This result is supported by the resistivity results where the resistivity of CaPr-doped Nd is larger the resistivity of CaTh doped Y. The inter-layer coupling, $J = [2\xi_c(0)]^2/d^2$, [3] was obtained. The J values are given in Table 1. The inter-layer-coupling are increase with increasing doping concentration. This means that the partial replacement RE ions by either CaPr or CaTh ions increase the CuO_2 inter-layer coupling. This leads to reduction of the effective layer thickness of the 2D system, d, and the wire cross-sectional area, s, of the 1D system as the substitution content increases.

The upper critical magnetic field at 0 K, $B_{c2}(0)$, calculated from the coherence length relations in the ab and c directions is given by [23, 24]

$$B_{c2,ab} = \frac{\Phi_0}{2\pi\xi_{ab}(0)\xi_c(0)} \tag{9}$$

$$B_{c2,c} = \frac{\Phi_0}{2\pi\xi_{ab}^2(0)} \tag{10}$$

where $\Phi_0 = h/2e$ is the flux-quantum number. B_{c2} versus doping level is shown in Fig. 4. B_{c2} is increased by increasing the doping. This originates from the decreased coherence length due to the introduction of disorder by doping.

The critical current density, J_c, is one of the most significant physical properties in high-T_c superconductors and is given for self-field at 0 K by [23, 24]

$$J_c = \frac{2\Phi_0}{\sqrt{6}\pi\lambda^2(0)\xi_c(0)} \tag{11}$$

where $\lambda(0)$ is the penetration depth at zero temperature and is about 150 nm in RE-123 superconductors [25]. Figure 5

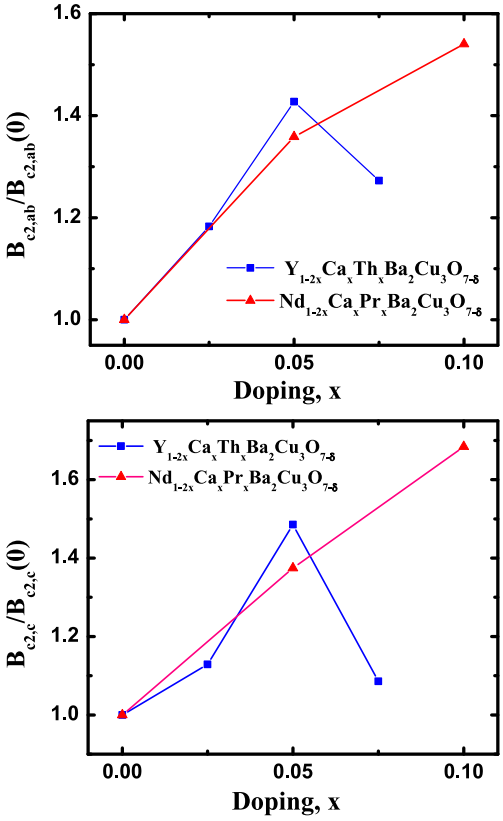

Fig. 4 The upper critical magnetic field normalized with respect to the undoped value at 0 K versus x in the ab and c directions

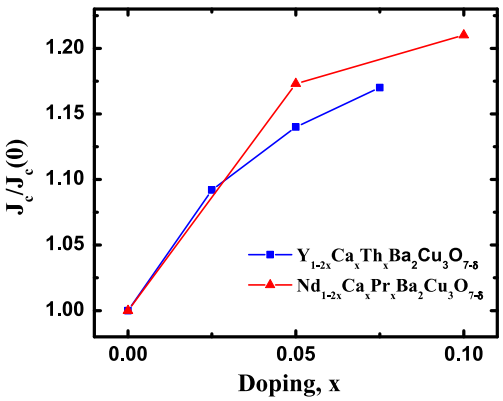

Fig. 5 The critical current density, normalized with respect to the value for the undoped sample at self field and 0 K, versus x

shows the critical current density versus doping level. J_c is increased by increasing the doping concentration x. The J_c is mainly controlled by flux pinning. The increase in J_c is most likely to be due to disorder introduced by doping. The increasing disorder due to the increasing doping concentration results in increasing pinning force. As can be seen in Fig. 5, the value of critical current density in Nd(CaPr)-123 is larger than Y(CaTh)-123 at higher doping concentration. This result suggests that the introduced pinning center by CaPr doping is more effective than CaTh.

5 Conclusions

The excess conductivity for $RE_{1-2x}Ca_xM_xBa_2Cu_3O_{7-\delta}$ with RE = Y, Nd and M = Th, Pr ($0.00 \leq x \leq 0.10$) were analyzed using the LD model. By calculating the coherence length in the ab and c directions, it is shown that the normalized coherence lengths were decreased by increasing doping, and therefore, the upper critical field and critical current density were increased. The crossover temperatures were found to shift to lower temperature values with increased doping, and the width of 3D region is decreased with increasing doping. It was found that the upper critical field and critical current density were increased with increasing doping concentration, which is due to the introduction of disorder and the enhancement of flux pinning by increasing charge neutral doping. The result shows that the introduced pinning center by CaPr doping is more effective than CaTh.

References

1. Bednorz, J.G., Muller, K.A.: Phys. Rev. B **64**, 189 (1986)
2. Aslamazov, L.G., Larkin, A.L.: Phys. Lett. A **26**, 238 (1968)
3. Lawrence, W.E., Doniach, S.: In: Kanada, E. (ed.) Proceedings of the Twelfth International Conference on Low Temperature Physics, Keigaku, Tokyo, p. 361 (1971)
4. Maki, K.: Prog. Theor. Phys. **39**, 897 (1968)
5. Thompson, R.S.: Phys. Rev. B **1**, 327 (1970)
6. Hikami, S., Larkin, A.I.: Mod. Phys. Lett. B **2**, 693 (1998)
7. Sharma, S.V., Sinha, G., Nath, T.K., Chakraborty, S., Majumdar, A.K.: Physica C **351**, 242 (1995)
8. Han, S.H., Rapp, Ö.: Solid State Commun. **94**, 661 (1995)
9. Mori, N.: Physica C **154**, 445 (2006)
10. Kim, H.J., Kim, K.H., Kang, W.N., Lee, H.S., Kim, K.H.P., Choi, E.M., Kim, H.J., Lee, S.I., Mun, M.O.: Physica C **408–410**, 72 (2004)
11. Khalil, S.M.: J. Low Temp. Phys. C **369**, 286 (2006)
12. Ghorbani, S.R., Andersson, M., Rapp, Ö.: Physica C **424**, 159 (2005)
13. Abou-Aly, A.I., Awad, R., Ibrahim, I.H., Abdeen, W.: Solid State Commun. **149**, 281 (2009)
14. Aslamasov, L.G., Larkin, A.I.: Sov. Phys., Solid State **10**, 875 (1968)
15. Pradhan, A.K., Roy, S.B., Chen, P., Waklyn, B.M.: Phys. Rev. B **50**, 7180 (1994)
16. Sharifi, F., Herzog, A.V., Dynes, R.C.: Phys. Rev. Lett. **71**, 428 (1993)
17. Konsin, P., Sorkin, B., Ausloos, M.: Supercond. Sci. Technol. **11**, 1 (1998)
18. Khan, N.A., Mumtaz, A.: Physica B **405**, 2772 (2010)
19. Rojas Sarmiento, M.P., Uribe Laverde, M.A., Vera Lopez, E., Landinez Tellez, D.A., Roa-Rojas, J.: Physica B **398**, 360 (2007)
20. Vovk, R.V., Obolenskii, M.A., Bondarenko, A.V., Goulatis, I.L., Chroneos, A.: Acta Phys. Pol. **111**, 129 (2007)

21. Han, S.H., Axnas, J., Zhao, B.R., Rapp, Ö.: Physica C **408–410**, 679 (2004). Physica C **390**, 160 (2003)
22. Lundqvist, P., Rapp, Ö., Tellgren, R., Bryntse, I.: Phys. Rev. B **56**, 2824 (1997)
23. Tinkham, M.: Physica C **235–240**, 3 (1994)
24. Charles Poole, P., Farach, A.H. Jr., Creswick, J.R., Prozorv, R.: Superconductivity, 2nd edn. Academic Press, San Diego (2007)
25. Athanassopoulou, N., Cooper, J.R.: Physica C **259**, 326 (1996)